



HAL
open science

Origin of the Large Anisotropic g Factor of Holes in Bismuth

Yuki Fuseya, Zengwei Zhu, Benoît Fauqué, Woun Kang, Bertrand Lenoir,
Kamran Behnia

► **To cite this version:**

Yuki Fuseya, Zengwei Zhu, Benoît Fauqué, Woun Kang, Bertrand Lenoir, et al.. Origin of the Large Anisotropic g Factor of Holes in Bismuth. *Physical Review Letters*, 2015, 115, pp.216401. 10.1103/PhysRevLett.115.216401 . hal-03984239

HAL Id: hal-03984239

<https://hal.univ-lorraine.fr/hal-03984239>

Submitted on 12 Feb 2023

HAL is a multi-disciplinary open access archive for the deposit and dissemination of scientific research documents, whether they are published or not. The documents may come from teaching and research institutions in France or abroad, or from public or private research centers.

L'archive ouverte pluridisciplinaire **HAL**, est destinée au dépôt et à la diffusion de documents scientifiques de niveau recherche, publiés ou non, émanant des établissements d'enseignement et de recherche français ou étrangers, des laboratoires publics ou privés.

Origin of the Large Anisotropic g Factor of Holes in Bismuth

Yuki Fuseya,^{1,*} Zengwei Zhu,² Benoît Fauqué,² Woun Kang,³ Bertrand Lenoir,⁴ and Kamran Behnia²

¹*Department of Engineering Science, University of Electro-Communications, Chofu, Tokyo 182-8585, Japan*

²*LPEM (UPMC-CNRS), Ecole Supérieure de Physique et de Chimie Industrielles, 75005 Paris, France*

³*Department of Physics, Ewha Womans University, Seoul 120-750, Korea*

⁴*Institut Jean Lamour (UMR 7198 CNRS, Nancy Université, UPVM), Ecole Nationale Supérieure des Mines de Nancy, 54042 Nancy, France*

(Received 20 July 2015; published 16 November 2015)

The ratio of the Zeeman splitting to the cyclotron energy ($M = \Delta E_Z / \hbar\omega_c$) for holelike carriers in bismuth has been quantified with great precision by many experiments performed during the past five decades. It exceeds 2 when the magnetic field is along the trigonal axis and vanishes in the perpendicular configuration. Theoretically, however, M is expected to be isotropic and equal to unity in a two-band Dirac model. We argue that a solution to this half-a-century-old puzzle can be found by extending the $\mathbf{k} \cdot \mathbf{p}$ theory to multiple bands. Our model not only gives a quantitative account of the magnitude and anisotropy of M for holelike carriers in bismuth, but also explains its contrasting evolution with antimony doping and pressure, both probed by new experiments reported here. The present results have important implications for the magnitude and anisotropy of M in other systems with strong spin-orbit coupling.

DOI: 10.1103/PhysRevLett.115.216401

PACS numbers: 71.18.+y, 71.55.Ak, 72.15.Jf

Spin-orbit interaction (SOI) is a central issue in contemporary solid state physics. It is an automatic consequence of the Dirac theory and well understood for a lonely electron in the presence of a single atomic potential. In crystals, however, a diversity of SOI effects arise due to a variety of crystalline potentials and the momentum of electrons. It is thus basically difficult to study the effect of SOI for various materials and various k points of the Brillouin zone by a universal approach.

One signature of crystalline SOI is its impact on the ratio of the Zeeman splitting ΔE_Z to the cyclotron energy $\hbar\omega_c$, dubbed $M \equiv \Delta E_Z / \hbar\omega_c$. The crystalline SOI appears as an antisymmetric part with respect to the commutation of momentum operators in the Hamiltonian under a magnetic field [1–6]. Its eigenvalue corresponds to the effective Zeeman energy with an anisotropic effective g factor \tilde{g} , while the eigenvalue of the symmetric part corresponds to the cyclotron energy with an anisotropic effective mass. Therefore, the impact of the crystalline SOI can be characterized by the relative energy scale of the crystalline SOI to the kinetic energy, i.e., $M = \Delta E_Z / \hbar\omega_c$. This ratio can be accurately determined by experiment in those cases in which quantum oscillations simultaneously detect successive Landau levels as well as same-index sublevels with opposite spins [7–14]. The energy levels for different cases and their corresponding M are illustrated in Fig. 1, and the experimental values of M in three different systems are listed in Table I. As seen in this table, when the SOI is weak, M is much smaller than unity. One can show that M is exactly equal to unity (and so never exceeds unity) for any direction of the magnetic field when a large SOI strongly couples two bands based on the two-band model,

which is equivalent to the Dirac Hamiltonian [3,5,6]. This agrees quite well with the experiments on the L point of bismuth, the typical Dirac electrons in solids.

However, in the case of holes at the T point, there are two puzzling features: (i) M is extremely anisotropic ($=0$ for a $B \perp$ trigonal axis); (ii) it largely exceeds unity in one configuration ($= 2.12$ for a $B \parallel$ trigonal axis) as shown later. These two puzzles emerged from numerous experiments starting half a century ago [18] in the absence of any satisfactory explanations [7–12]. In other words, the two-band approach completely fails to give its adequate value.

In this Letter, we show that a satisfactory solution to these long-standing puzzles can be found by going beyond the two-band Dirac model. Furthermore, we present new experimental results on the evolution of M for holes in bismuth with pressure and antimony substitution. Rather counterintuitively, these two alternative ways to reduce carrier concentration shift the magnitude of M in opposite

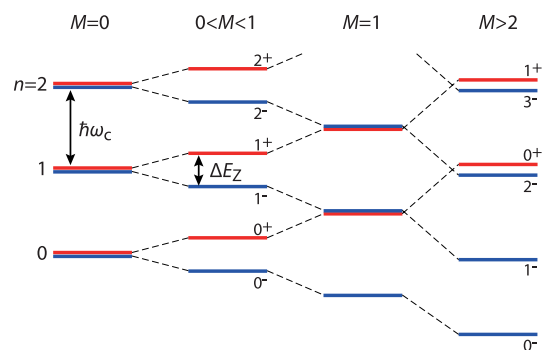


FIG. 1 (color online). Energy levels under a magnetic field for different ratios $M = \Delta E_Z / \hbar\omega_c$.

TABLE I. Ratio M for some compounds. The cyclotron mass [2,11,15,16], g factor [2,11,16,17], and atomic SOI [4] are also listed. For graphite, only values with the magnetic field parallel to the c axis are listed. The range of values for Bi expresses their anisotropy.

	Graphite		InSb	Bi	
Position	K (ele.)	H (hole)	Γ	L (ele.)	T (hole)
m_c/m	0.038	0.057	0.014	0.0019–0.027	0.068–0.22
\tilde{g}	2.5	2.5	52	74–1060	0.79–63
$M = m_c \tilde{g}/2m$	0.048	0.073	0.36	0.9–1.0	0.0–2.12
Atomic SO (eV)	0.005	0.005	0.27, 0.68	1.8	1.8

directions. We show that this can be quantitatively explained by the present approach.

Numerous experiments have quantified the magnitude of the g factor and M for both electrons and holes in bismuth [7–12]. The large atomic SOI (~ 1.8 eV) overwhelmingly dominates all other energy scales including the Fermi energy (≈ 28 meV) and the band gap (≈ 15 meV). Therefore, the crystalline SOI dramatically affects the electronic structure, and this leads to a very complex hierarchy between $\hbar\omega_c$ and ΔE_Z for different carriers and different orientations of the magnetic field. In the case of electrons at the L point, $M \approx 1$ with little dependence on the field orientation. In other words, in spite of the extreme anisotropy of both the cyclotron mass m_c and \tilde{g} [11], $\hbar\omega_c$ and ΔE_Z remain almost equal to each other. This property of the L electrons is quite well understood based on the two-band model [3,5,6], which was employed to give a quantitative account of the complex Landau spectrum of L electrons [11,12]. The puzzling features experimentally observed on holes at the T point are shown in Fig. 2, which shows the angular dependence of two Nernst peaks corresponding to energy levels $n = 2^\pm$, where \pm indicates the degree of freedom of the Kramers doublet [12]. The angular dependence of M can be deduced by plotting $F_{\text{tri}}^{-1}(B^{2+} - B^{2-})$, which is shown also in Fig. 2, where B^{2^\pm} is the magnetic field of the Nernst peak for $n = 2^\pm$ and F_{tri} is the oscillation frequency for a $B||$ trigonal axis. For $B||$ trigonal, this value is exactly the same as M , and so

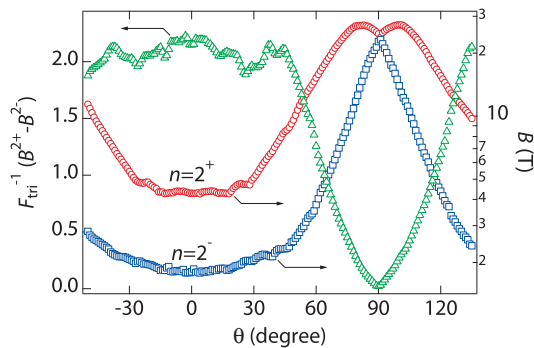


FIG. 2 (color online). Angular dependence of two Nernst peaks for $n = 2^+$, 2^- on bismuth (from Ref. [12]) and $F_{\text{tri}}^{-1}(B^{2+} - B^{2-})$. θ is the angle between the magnetic field and the trigonal axis.

we obtain $M = 2.12$ (cf. Fig. 1). For $B \perp$ trigonal, on the other hand, $F_{\text{tri}}^{-1}(B^{2+} - B^{2-})$ becomes almost zero, indicating $M \approx 0$.

Next, we give a general theory on the ratio M . We start from a one-electron Hamiltonian in the presence of a strong SOI and apply the $\mathbf{k} \cdot \mathbf{p}$ theory to a multiband system under a magnetic field taking into account the SOI in a fully relativistic (nonperturbative) way. The theoretical concepts used here are orthodox, but for the first time they are employed to give a quantitative description of a nontrivial M in a well-characterized solid.

The obtained Hamiltonian is written in terms of a $2n \times 2n$ matrix for an n -band system [18]. In order to study the electromagnetic properties of electrons belonging to a particular band, we decouple the 2×2 Hamiltonian $\mathcal{H}_{n=0}$ from the other bands by using Löwdin's unitary transformation [21]. The cyclotron energy is the eigenvalue of the symmetric part of $\mathcal{H}_{n=0}$. A straightforward calculation yields $\hbar\omega_c = (e\hbar B/c)\sqrt{\det \alpha(\alpha^{-1})_{ii}}$, where α is the inverse mass tensor given by

$$\alpha_{ij} = \frac{\delta_{ij}}{m} + \sum_{n \neq 0} \frac{t_{ni}t_{nj}^* + t_{nj}t_{ni}^* + u_{ni}u_{nj}^* + u_{nj}u_{ni}^*}{E_0 - E_n}. \quad (1)$$

We have extended the notations of Cohen-Blount as $\mathbf{t}_n = \mathbf{v}_{0n}^{\uparrow\uparrow}$ and $\mathbf{u}_n = \mathbf{v}_{0n}^{\uparrow\downarrow}$, where $v_{ij}^{\zeta\eta}$ is the interband matrix element of the velocity operator between the i th band with spin ζ and the j th band with spin η . E_Z is given as the eigenvalue of the antisymmetric part of $\mathcal{H}_{n=0}$. For $\mathbf{B}||i$, it is obtained as $E_Z = \pm(\tilde{g}/2)\mu_B B_i$, where $\tilde{g} = 2m\sqrt{G_{ii}}$,

$$G_{ii} = 4 \left| \left(\sum_{n \neq 0} \frac{\mathbf{t}_n \times \mathbf{u}_n}{E_0 - E_n} \right)_i \right|^2 - \left(\sum_{n \neq 0} \frac{\mathbf{t}_n \times \mathbf{t}_n^* + \mathbf{u}_n \times \mathbf{u}_n^*}{E_0 - E_n} \right)_i^2, \quad (2)$$

and $\mu_B = e\hbar/2mc$. Then, M for $B||z$ is

$$M = \frac{\Delta E_Z}{\hbar\omega_c} = \sqrt{\frac{G_{zz}}{\alpha_{xx}\alpha_{yy} - \alpha_{xy}^2}}. \quad (3)$$

The obtained results (1)–(3) are all gauge independent. It should be stressed that the denominators $E_0 - E_n$ of α and G approximately canceled each other in M . Therefore, M is very sensitive to the symmetric properties of the interband matrix elements and insensitive to the energy differences. In the case with a strong SOI, the $1/m$ term in Eq. (1) is negligibly small. We will generally discard it hereafter. If only two bands ($n = 0, 1$) are taken into account for the strongly spin-orbit coupled systems, $G_{zz} = \alpha_{xx}\alpha_{yy} - \alpha_{xy}^2$, and then M would be exactly unity, consistent with previous results [3,5,6].

Various theories of \tilde{g} for multiband systems have been studied so far. The simple formula available at the present moment is valid only in the semiclassical limit [22], whereas the formulas for Bloch bands based on the quantum treatment are too complex to compute \tilde{g} for various systems [4,23,24]. The present quantum formulas for $\hbar\omega_c$, \tilde{g} , and M are general, rigorous within the $\mathbf{k} \cdot \mathbf{p}$ theory, and yet easy to handle. It is the advantage of these formulas that these values can be automatically obtained from the interband matrix elements and the energy differences, which can be directly computed by the band calculations as shown later.

Here we give a concrete example of the above theory. We adopt obtained formulas to the T -point holes in bismuth by taking into account the symmetry at the T point. As is well known, bismuth is a very good test material for various aspects of electronic physics [6,25]. Actually, the following arguments are also valid for group V semimetals (Sb, As), IV–VI narrow gap semiconductors (PbTe, PbSe, SnTe, etc.), and the topological insulator Bi_2Se_3 , since the k points where their carrier locate have the same symmetry as the T point of bismuth [26,27]. The hole band at the T point of bismuth has the symmetry of T_{45}^- [28,29]. The symmetries of the other bands at the T points are shown in Fig. 4(e) and Fig. 1 in Supplemental Material [18]. (The group theoretical notation is that of Ref. [29].) From the selection rules, the matrix elements between the T_{45}^- band and the others are finite only for $\mathbf{t}_n^{(6)} = \langle T_{45}^-(1) | \mathbf{v} | T_6^+(n) \rangle = (-a_n, ia_n, 0)$, $\mathbf{u}_n^{(6)} = \langle T_{45}^-(1) | \mathbf{v} | CT_6^+(n) \rangle = (-a_n, -ia_n, 0)$, and $\mathbf{u}_n^{(45)} = \langle T_{45}^-(1) | \mathbf{v} | CT_{45}^+(n) \rangle = (0, 0, b_n)$, where C is the product of space inversion and time-reversal operators and a_n , b_n are complex numbers [29]. The x , y , and z directions are taken along the binary, bisectrix, and trigonal axes, respectively. Since \tilde{g} is given by the outer products of \mathbf{t}_n and \mathbf{u}_n [Eq. (2)], it is clear from $\mathbf{t}_n^{(6)}$ and $\mathbf{u}_n^{(45)}$ that G_{zz} is the only nonvanishing term. Therefore, the angular dependence of ΔE_Z is simply $\Delta E_Z(\theta) = 2m\mu_B B |\cos\theta| \sqrt{G_{zz}}$, where θ quantifies the tilt angle of the magnetic field off the trigonal axis. This leads to $\tilde{g} = 0$ for a $B \perp$ trigonal axis, providing a solution to the first experimental puzzle.

The ratio M for the T -point holes is obtained as

$$M = \sqrt{\left| \sum_{n \neq 0} \frac{a_n^2}{E_0 - E_n} \right|^2 / \left(\sum_{n \neq 0} \frac{|a_n|^2}{E_0 - E_n} \right)^2}. \quad (4)$$

This form makes it easy to understand how M can exceed unity. For example, in the case with three bands $n = 0, 1, 2$, whose energies are $E_2 < E_0 < E_1$, it is easy to show that the ratio is always greater than one *no matter how large the energy differences are* [Eq. (32) in [18]]. Accordingly, one expects that the interband contributions from the lower (higher) energy bands increase (decrease) the ratio, providing a possible solution to the second experimental puzzle.

In order to know the definite value of M , we need to evaluate the interband matrix elements \mathbf{t}_n , \mathbf{u}_n and the energy differences $E_0 - E_n$ based on the band calculations. Here we evaluate them based on the multiband $\mathbf{k} \cdot \mathbf{p}$ Hamiltonian (eight-band model) derived from the well-known tight-binding band calculation of Bi by Liu and Allen, which is in quantitative agreement with experiments [30]. Then, by using the obtained formulas for α_{ij} , \tilde{g} , and M , they can be automatically obtained as $\alpha_{xx} = \alpha_{yy} = 14.1$, $\alpha_{xy} = 0$, $\tilde{g} = 58.7$, and $M = 2.08$ for $B \parallel$ trigonal, which agrees well with the experimental value of 2.12. The only band that can increase M is $T_6^+(2)$ (Fig. 1 in [18]). Therefore, and surprisingly, a band 1 eV far from the band in which carriers resides can enhance the magnitude of M by a factor of 2. This large interband effect provides a quantitative solution to the second puzzle.

An additional cross-check is provided by the evolution of M with alloying [31] or by applying pressure. One may naively expect that substituting bismuth with antimony can be assimilated to chemical pressure and therefore the results should be identical to applying physical pressure. But there are two essential differences. First, the substitution changes the strength of the SOI, while the pressure does not. Second, the lattice structure becomes more rhombohedral by substitution [32], while it tends to approach cubic by the pressure [33]. Figure 3 shows the Nernst signal of Bi as a function of FB^{-1} for pure Bi at $P = 0$, $\text{Bi}_{0.96}\text{Sb}_{0.04}$ alloy at $P = 0$, and pure Bi at $P = 1.37$ GPa [18]. We can distinguish the peaks of $n = 0^+$ and 2^- from their different temperature dependence. In the case of Sb substitution, the 0^+ and 2^- peaks shift, but the order is unchanged. Applying pressure, on the other hand, inverts the order. This difference can be seen by plotting M as a function of Sb content and pressure shown in Figs. 4(a) and 4(b), respectively. M increases with substitution but decreases with pressure. Note that in both cases, as shown in Figs. 4(c) and 4(d), the frequency of quantum oscillations decreases as was found before [34,35]. This implies that the Fermi surface shrinks because the overlap between the conduction band at the L point and the valence band at the T point is reduced.

These experimental results can be naturally interpreted by the present theory in terms of the relevance of the

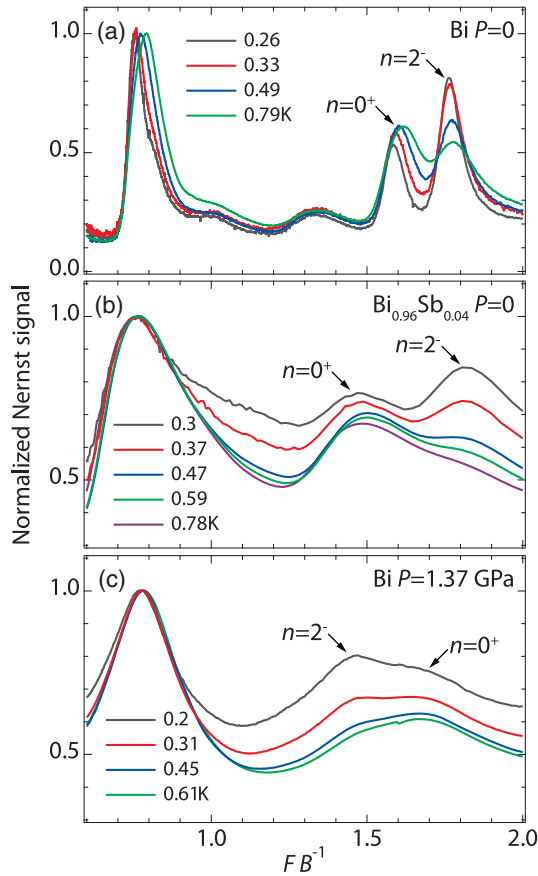


FIG. 3 (color online). Nernst signal as a function of FB^{-1} at different temperatures for (a) pure Bi at $P = 0$, (b) Bi with 4% Sb substitution at $P = 0$, and (c) pure Bi at $P = 1.37$ GPa. The magnetic field is along the trigonal axis, and F is the frequency of the quantum oscillation.

interband contributions. Figures 4(e) and 4(f) show the theoretically obtained energy differences from the hole band (T_{45}^-) with respect to the Sb content and the compression in volume, $-\Delta\Omega/\Omega_0$, respectively. ($-\Delta\Omega/\Omega_0 = 0.041$ corresponds to 1.5 GPa [36].) In the case of the substitution, both the higher energy $T_6^+(3)$, $T_{45}^+(1)$ and the lower energy $T_6^+(2)$ go up, so that the contribution from the lower energy band increases resulting in the enhancement of M shown by lines in Fig. 4(a). In the case of pressure, on the other hand, both the higher and lower bands move downward, so that the contribution from the higher energy band increases resulting in the decrease of M shown in Fig. 4(b). Even though the energy shifts are very small, they make a sizable change in M . In both cases, the overlap between the L -conduction and T -valence bands decreases as shown in the insets in Figs. 4(c) and 4(d). As seen in the figure, there is satisfactory agreement between the theory and experiment. For Sb substitution, we adopt a simple virtual crystal approximation [37]. As for pressure, we assume that the overlap integrals scale with d^{-2} , where d is the bond length [18,30].

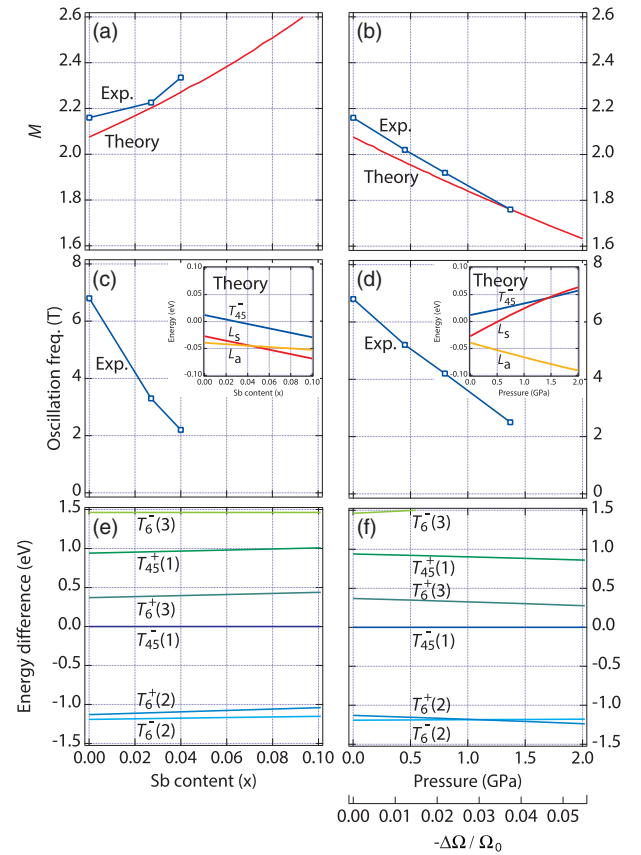


FIG. 4 (color online). The ratio M [(a),(b)], the quantum oscillation frequency [(c),(d)], and the energy differences from the hole band (T_{45}^-) [(e),(f)] as a function of Sb content (left column) and pressure (right column). The insets in (c) and (d) are the energy shift of the T -point hole band, the conduction, and valence band at the L point, taken the origin of the energy as the position of the Fermi energy of pure Bi at $P = 0$.

In summary, we studied the ratio of the Zeeman splitting to the cyclotron energy and derived a new formula based on the multiband $\mathbf{k} \cdot \mathbf{p}$ theory. This provides an explanation for the large and anisotropic ratio, which is beyond the two-band Dirac approach. New experimental results on antimony substitution and pressure are in quantitative agreement with the present theory. Beyond the specific case of bismuth, this general scheme can be applied to materials where a SOI plays a relevant role, including IV–VI semiconductors (PbTe, SbSe, SnTe), and topological insulators such as Bi₂Se₃ in which experiment indicates $M \sim 2$ [13,14,38].

We thank K. Abe, H. Harima, K. Hattori, and H. Kusunose for helpful discussions. Y.F. is supported by JSPS KAKENHI Grants No. 24244053 and No. 25870231. B.F. and K.B. are supported by Agence Nationale de la Recherche through SUPERFIELD and QUANTUM LIMIT projects. W.K. is supported by the NRF grants funded by the Korea Government (MSIP) (No. 2015-001948 and No. 2010-00453).

- *fuseya@pc.uec.ac.jp
- [1] J. M. Luttinger, *Phys. Rev.* **102**, 1030 (1956).
- [2] L. M. Roth, B. Lax, and S. Zwerdling, *Phys. Rev.* **114**, 90 (1959).
- [3] M. H. Cohen and E. I. Blount, *Philos. Mag.* **5**, 115 (1960).
- [4] Y. Yafet, *Solid State Phys.* **14**, 1 (1963).
- [5] P. A. Wolff, *J. Phys. Chem. Solids* **25**, 1057 (1964).
- [6] Y. Fuseya, M. Ogata, and H. Fukuyama, *J. Phys. Soc. Jpn.* **84**, 012001 (2015).
- [7] G. E. Smith, G. A. Baraff, and J. M. Rowell, *Phys. Rev.* **135**, A1118 (1964).
- [8] V. S. Édel'man, *Adv. Phys.* **25**, 555 (1976).
- [9] S. G. Bompadre, C. Biagini, D. Maslov, and A. F. Hebard, *Phys. Rev. B* **64**, 073103 (2001).
- [10] K. Behnia, M.-A. Méasson, and Y. Kopelevich, *Phys. Rev. Lett.* **98**, 166602 (2007).
- [11] Z. Zhu, B. Fauqué, Y. Fuseya, and K. Behnia, *Phys. Rev. B* **84**, 115137 (2011).
- [12] Z. Zhu, B. Fauqué, L. Malone, A. B. Antunes, Y. Fuseya, and K. Behnia, *Proc. Natl. Acad. Sci. U.S.A.* **109**, 14813 (2012).
- [13] H. Kohler and E. Wuchener, *Phys. Status Solidi (b)* **67**, 665 (1975).
- [14] B. Fauqué, N. P. Butch, P. Syers, J. Paglione, S. Wiedmann, A. Collaudin, B. Grenn, U. Zeitler, and K. Behnia, *Phys. Rev. B* **87**, 035133 (2013).
- [15] D. E. Soule, J. W. McClure, and L. B. Smith, *Phys. Rev.* **134**, A453 (1964).
- [16] A. V. Vdovin and E. M. Skok, *Phys. Status Solidi (b)* **136**, 603 (1986).
- [17] J. M. Schneider, N. A. Goncharuk, P. Vašek, P. Svoboda, Z. Výborný, L. Smrčka, M. Orlita, M. Potemski, and D. K. Maude, *Phys. Rev. B* **81**, 195204 (2010).
- [18] See Supplemental Material at <http://link.aps.org/supplemental/10.1103/PhysRevLett.115.216401>, which includes Refs. [19, 20], for details of the multiband $k \cdot p$ theory and experiments with antimony doping and pressure.
- [19] J. Alicea and L. Balents, *Phys. Rev. B* **79**, 241101(R) (2009).
- [20] A. Demouge, B. Lenoir, Y. I. Ravich, H. Scherrer, and S. Scherrer, *J. Phys. Chem. Solids* **56**, 1155 (1995).
- [21] R. Winkler, *Spin-Orbit Coupling Effects in Two-Dimensional Electron and Hole Systems* (Springer-Verlag, Berlin, 2003).
- [22] G. P. Mikitik and Y. V. Sharlai, *Phys. Rev. B* **65**, 184426 (2002).
- [23] E. I. Blount, *Phys. Rev.* **126**, 1636 (1962).
- [24] L. Roth, *J. Phys. Chem. Solids* **23**, 433 (1962).
- [25] L. A. Falkovskii, *Sov. Phys. Usp.* **11**, 1 (1968).
- [26] J. O. Dimmock and G. B. Wright, *Phys. Rev.* **135**, A821 (1964).
- [27] H. Zhang, C.-X. Liu, Z.-L. Qi, X. Dai, Z. Fang, and S.-C. Zhang, *Nat. Phys.* **5**, 438 (2009).
- [28] S. Mase, *J. Phys. Soc. Jpn.* **13**, 434 (1958).
- [29] S. Golin, *Phys. Rev.* **166**, 643 (1968).
- [30] Y. Liu and R. E. Allen, *Phys. Rev. B* **52**, 1566 (1995).
- [31] B. Lenoir, M. Cassart, J.-P. Michenaud, H. Scherrer, and S. Scherrer, *J. Phys. Chem. Solids* **57**, 89 (1996).
- [32] M. S. Dresselhaus, in *The Physics of Semimetals and Narrow Gap Semiconductors*, edited by D. L. Carter and R. T. Bate (Pergamon, New York, 1971), p. 3.
- [33] K. Aoki, S. Fujiwara, and M. Kusakabe, *J. Phys. Soc. Jpn.* **51**, 3826 (1982).
- [34] N. B. Brandt and S. M. Chudinov, *Sov. Phys. JETP* **32**, 815 (1971).
- [35] A. Banerjee, B. Fauqué, K. Izawa, A. Miyake, I. Sheikin, J. Flouquet, B. Lenoir, and K. Behnia, *Phys. Rev. B* **78**, 161103 (2008).
- [36] A. A. Giardini and G. A. Samara, *J. Phys. Chem. Solids* **26**, 1523 (1965).
- [37] J. C. Y. Teo, L. Fu, and C. L. Kane, *Phys. Rev. B* **78**, 045426 (2008).
- [38] M. Orlita, B. A. Piot, G. Martinez, N. K. Sampath Kumar, C. Faugeras, M. Potemski, C. Michel, E. M. Hankiewicz, T. Brauner, C. Drašar, S. Schreyeck, S. Grauer, K. Brunner, C. Gould, C. Brüne, and L. W. Molenkamp, *Phys. Rev. Lett.* **114**, 186401 (2015).